Supplementary Information

Metal-Free Approach to Bipyridinium Salt-Based

Conjugated Porous Polymers with Olefin Linkages

Jiawei Lin,[a] Shuai Bi,[*b] Zhongxiong Fan,[a] Zhenzhen Fu,[b] Zhaohui Meng,[a] Zhenqing Hou,[a] and Fan Zhang[*b]

a. College of Materials and Fujian Provincial Key Laboratory of Materials Genome, Xiamen University, Xiamen 361005, China.
b. School of Chemistry and Chemical Engineering, State Key Laboratory of Metal Matrix Composites, Shanghai Electrochemical Energy Devices Research Center, Shanghai Jiao Tong University, 800 Dongchuan Road, 200240 Shanghai, China.

Contents

1. Materials and Methods.

Materials.

1,3,5-tris(4-formylphenyl)-benzene (TFPB),[1, 2] 2,4,6-tris(4-formylphenyl)-1,3,5-triazine (TFPT),[3, 4] and 1,3,6,8-tetrakis(4-formylphenyl)-pyrene (TFPP)[5, 6] were prepared using reported methods. Triphenylamine, phosphorous oxychloride (POCl$_3$), Nickel(Ⅱ) chloride hexahydrate (NiCl$_2$·6H$_2$O), triphenylphosphine (PPh$_3$) and zinc were purchased from Macklin. Super dry DMF, 2-methyl-5-bromopyridine were purchased from J&K. All the other solvents mentioned were purchased from Adamas-beta Reagent and used without further purification.

Synthesis of 1,3,5-tris(4-formylphenyl)-amine (TFPA)[7, 8]
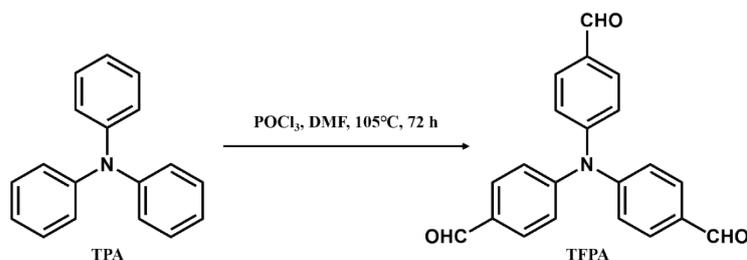
DMF (36 mL, 460.0 mmol) was ice-bathed and phosphorous oxychloride (47 mL, 500.0 mmol) was added dropwise. After stirring at 0 ℃ for 1 h, the temperature was allowed to warm to room temperature. Then triphenylamine (4.91 g, 20.0 mmol) was added and the mixture was stirred at 105 ℃ under which the phosphorous oxychloride will boil and reflux. After 72 h, the mixture was cooled to room temperature, poured into cold water and neutralized to pH=7-8 with 20% NaOH aqueous solution. After extraction with CH$_2$Cl$_2$ (3× 150 mL), the organic layer was washed with brine (3× 50 mL), dried with anhydrous sodium sulfate and filtered. After evaporation of the solvent, the crude product was purified by column chromatography using petroleum ether and ethyl acetate mixed solvent (3:1). Yield: 2.43 g (7.4 mmol, 36.9%).

^{1}H NMR (400 MHz, CDCl$_3$) δ (ppm): 9.95 (s, 1H), 7.84 (d, J = 7.8 Hz, 2H), 7.25 (d, J = 8.1 Hz, 2H).

Preparation of 1,1',6,6'-tetramethyl-3,3'-bipyridine (TMBP) [9]

5-bromo-2-methylpyridine   DMBP
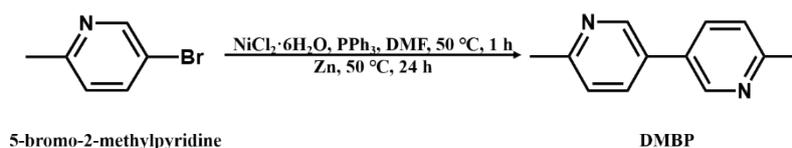
Nickel(II) chloride hexahydrate (14.26 g, 60.0 mmol), triphenylphosphine (62.95 g, 240.0 mmol), and 300 mL of DMF were introduced into a Schlenk flask. After bubbling nitrogen 0.5 h to deoxygenate the reaction system, the resulting deep blue solution was stirred for another 1 h at 50 °C. Then 3.92 g of zinc powder (60.0 mmol) was added. After 3 h, the color of the mixture changed to red brown, 10.32 g of 2-methyl-5-bromopyridine (60.0 mmol) was added and the temperature was allowed to rise to 75 °C and keep for 20 h. The mixture was added into the dilute aqueous ammonia (300 mL) and left until effervescence finished. Then the aqueous layer was extracted with dichloromethane (5 × 100 mL), the organic layer was extracted again with 2 M HCl solution (4 × 100 mL). The aqueous phase was neutralized with 4 M NaOH solution and extracted once again with dichloromethane (4 × 100 mL). After evaporation of the dichloromethane, the crude product was obtained to yield 6,6'-dimethyl-3,3'-bipyridine (DMBP). Yield: 3.32 g (18.0 mmol, 60.0%).

Synthesis of 1,1',6,6'-tetramethyl-[3,3'-bipyridine]-1,1'-diium iodide (TMBPI) [10]

DMBP   TMBPI

A solution of 6,6'-dimethyl-3,3'-bipyridine (0.92 g, 5.0 mmol) and iodomethane (3 mL, 10 equiv.) in CH_3CN (50 mL) was heated at 80 °C for 2 weeks. The mixture was filtered and the residue was washed with ethyl acetate, CH_2Cl_2, and acetone. Yield: 2.22 g (4.7 mmol, 94.9%). ^{1}H-NMR (400 MHz, D_2O) δ (ppm): 9.21 (s, 1H), 8.71 (d, J = 8.1 Hz, 1H), 8.10 (d, J = 8.2 Hz, 1H), 4.35 (s, 3H), 2.88 (s, 3H). ^{13}C NMR (101 MHz, D_2O) δ (ppm): 157.14, 144.43, 143.40, 131.63, 130.17, 46.24, 19.91.

Synthesis of TMBPI-TFPA:
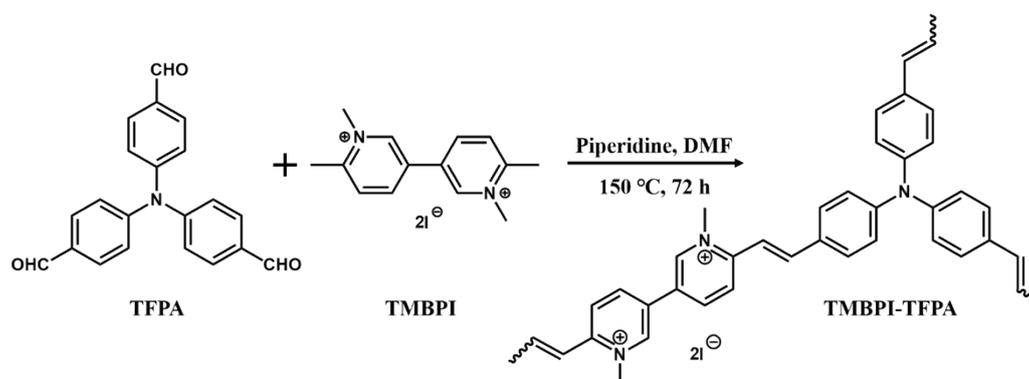
All CMPs were prepared under similar conditions. TMBPI-TFPA was synthesized through Knoevenagel condensation reaction between 1,3,5-tris(4-formylphenyl)-amine (TFPA, 66.0 mg, 0.2 mmol) and 1,1',6,6'-tetramethyl-[3,3'-bipyridine]-1,1'-diium iodide (TMBPI, 140.6 mg, 0.3 mmol) in super dry DMF (10 mL) at 150 ℃ catalyzed by piperidine (110 μL, 1.2 mmol, 2 equivalents to -CHO) in a sealed pressure vial under an argon atmosphere for 72 hours. The product was washed with DMF (2×15 mL), 3 M HCl aqueous (2×15 mL), deionized water (2×15 mL), ethyl acetate (2×15 mL), DCM (2×15 mL), MeOH (2×15 mL) and dried under vacuum at 80 ℃ for 12 h to afford the product in a yield of 96.2% (188.5 mg).

Synthesis of TMBPI-TFPB:
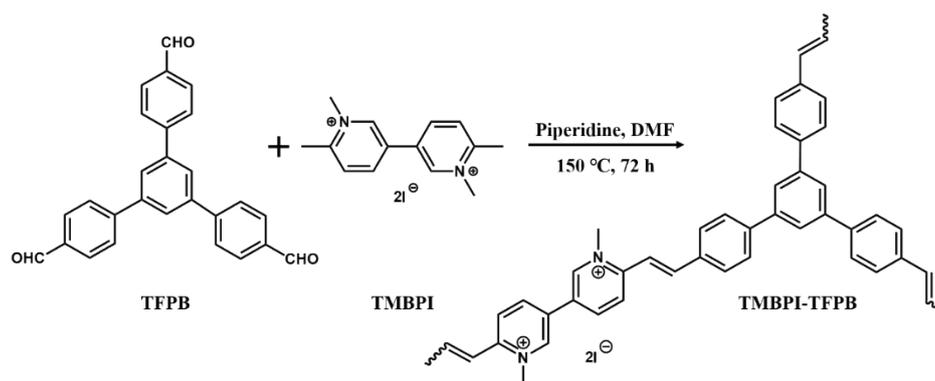
TMBPI-TFPB was synthesized through Knoevenagel condensation reaction between 1,3,5-tris(4-formylphenyl)-benzene (TFPB, 78.1 mg, 0.2 mmol) and 1,1',6,6'-tetramethyl-[3,3'-bipyridine]-1,1'-diium iodide (TMBPI, 140.6 mg, 0.3 mmol) in super dry DMF (10 mL) at 150 ℃ catalyzed by piperidine (110 μL, 1.2 mmol, 2 equivalents

to -CHO) in a sealed pressure vial under an argon atmosphere for 72 hours. The product was washed with DMF (2×15 mL), 3 M HCl aqueous (2×15 mL), deionized water (2×15 mL), ethyl acetate (2×15 mL), DCM (2×15 mL), MeOH (2×15 mL) and dried under vacuum at 60 ℃ for 12 h to afford the product in a yield of 81.8% (169.8 mg).

Synthesis of TMBPI-TFPT:
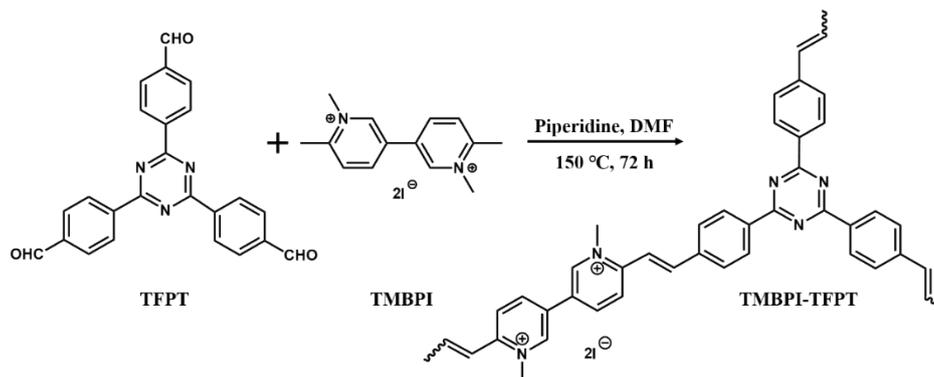
TMBPI-TFPT was synthesized through Knoevenagel condensation reaction between 2,4,6-tris(4-formylphenyl)-1,3,5-triazine (TFPT, 78.6 mg, 0.2 mmol) and 1,1',6,6'-tetramethyl-[3,3'-bipyridine]-1,1'-diium iodide (TMBPI, 140.6 mg, 0.3 mmol) in super dry DMF (10 mL) at 150 ℃ catalyzed by piperidine (110 μL, 1.2 mmol, 2 equivalents to -CHO) in a sealed pressure vial under an argon atmosphere for 72 hours. The product was washed with DMF (2×15 mL), 3 M HCl aqueous (2×15 mL), deionized water (2×15 mL), ethyl acetate (2×15 mL), DCM (2×15 mL), MeOH (2×15 mL) and dried under vacuum at 60 ℃ for 12 h to afford the product in a yield of 80.5% (167.7 mg).

Synthesis of TMBPI-TFPP:
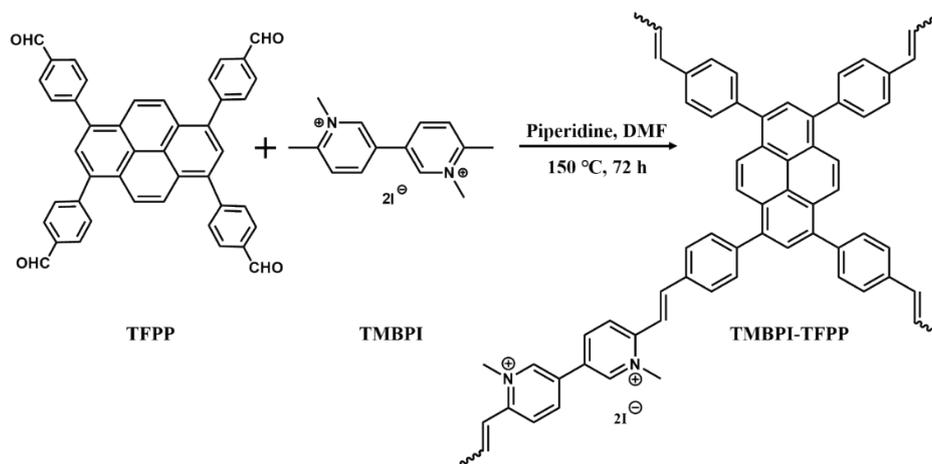
TMBPI-TFPP was synthesized through Knoevenagel condensation reaction between 1,3,6,8-tetrakis(4-formylphenyl)-pyrene (TFPP, 93.1 mg, 0.15 mmol) and 1,1',6,6'-tetramethyl-[3,3'-bipyridine]-1,1'-diium iodide (TMBPI, 140.6 mg, 0.30 mmol) in super dry DMF (10 mL) at 150 ℃ catalyzed by piperidine (110 μL, 1.2 mmol, 2 equivalents to -CHO) in a sealed pressure vial under an argon atmosphere for 72 hours. The product was washed with DMF (2×15 mL), 3 M HCl aqueous (2×15 mL), deionized water (2×15 mL), ethyl acetate (2×15 mL), DCM (2×15 mL), MeOH (2×15 mL) and dried under vacuum at 60 ℃ for 12 h to afford the product in a yield of 65.5% (146.2 mg).

2. Characterization

The reactions involving inert atmosphere were carried out using standard Schlenk technique or in an MBraun glovebox.

The structures of monomers and polymers were characterized by a Fourier transform infrared (FT-IR) spectrometer (Nicolet iS10). FT-IR spectra were collected in the wavenumber range of 450 ~ 4000 cm^{-1} using the KBr pallet.

The solution nuclear magnetic resonance (NMR) spectra were recorded at ambient temperature on Mercury plus 400 (400 MHz for proton, 100 MHz for carbon) spectrometer with tetramethyl silane as the internal reference using CDCl$_3$ or D$_2$O as solvent. And solid state ^{13}C cross-polarization/magic angle spinning (CP/MAS) NMR spectra were recorded on WB 400 MHz BRUKER AV III spectrometer. Measurements were made with a 4 mm MAS probe spinning at 10 kHz.

X-ray photoelectron spectroscopy (XPS) was carried out on Thermo Fisher ESCALAB 250Xi spectrometer to investigate the chemical structure of the porous polymers with Al Kα excitation radiation, the C 1s was valued at 284.8 eV for charge corrections.

The Powder X-Ray Diffraction (PXRD) patterns were recorded on a Bruker-Axe X-ray diffractometer by Cu kα radiation source (40 kV, 40 mA, λ= 0.0163 nm).

Thermal gravimetric analyses (TGA) were conducted using a thermal analyzer (NETZSCH STA 449F3) under a N_2 atmosphere from ambient temperature to 800 ℃ with a heating rate of 10 °C min^{-1}.

Nitrogen adsorption-desorption isotherms were performed at 77.3 K on a Micromeritics Tristar II 3020 equipment. Prior to adsorption measurements, the porous polymers were degassed for 12 h at 120 °C to ensure that the residual pressure fell below 10 mbar. The BET surface areas were calculated within the relative pressure range of 0.05 to 0.2. Pore size distributions were achieved by applying the nonlocal density functional theory model to the adsorption isotherms. The total volume was calculated at $P/P_0 = 0.99$.

The morphologies of the porous polymers were investigated by scanning electron microscopy (SEM) (SU-70, Hitachi) with an accelerating voltage of 10 kV and a working distance of 15 mm and transmission electron microscope (TEM) (Talos F200X) with an accelerating voltage of 200 kV.

The antimicrobial property is reflected on the number of colony-forming units (CFU). Antimicrobial property evaluation of each sample was performed by exposure to Gram-positive S. *aureus* ($1.10×10^6$ CFU/mL) and Gram-negative E. *coli* ($1.05×10^6$ CFU/mL). Briefly, 10 mg sample was suspended in 50 mL PBS solution with ultrasonication. Then 2 mL of bacteria suspension was added into 2 mL of the above PBS solution. The mixture was incubated in shaking incubator at 37 ℃. After 12 h, The solution was diluted and 200 μL of each dilution was dispersed on trypticase agar plates. The colony-forming units (CFU) of bacteria on the agar plates were counted after incubation at 37 ℃ for 12 h. The test was repeated three times to obtain the average results.

3. NMR Spectra of monomers
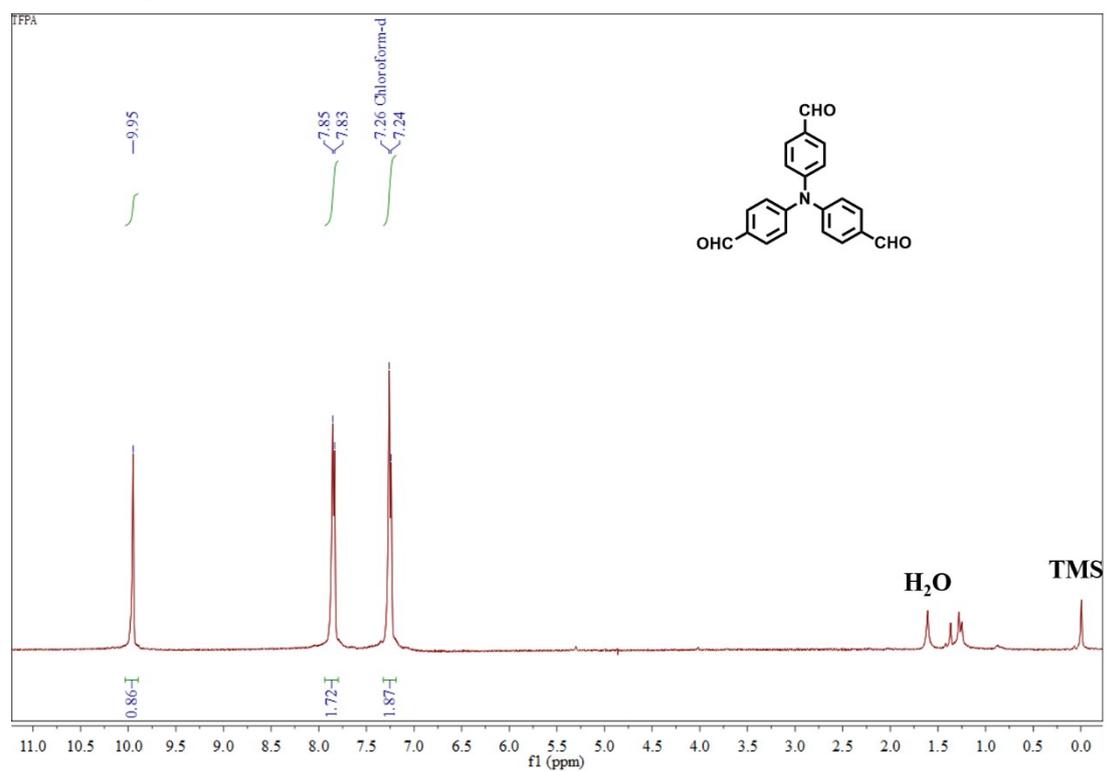
Fig. S1 ^{1}H NMR of 1,3,5-tris(4-formylphenyl)-amine (TFPA) recorded in CDCl$_3$.
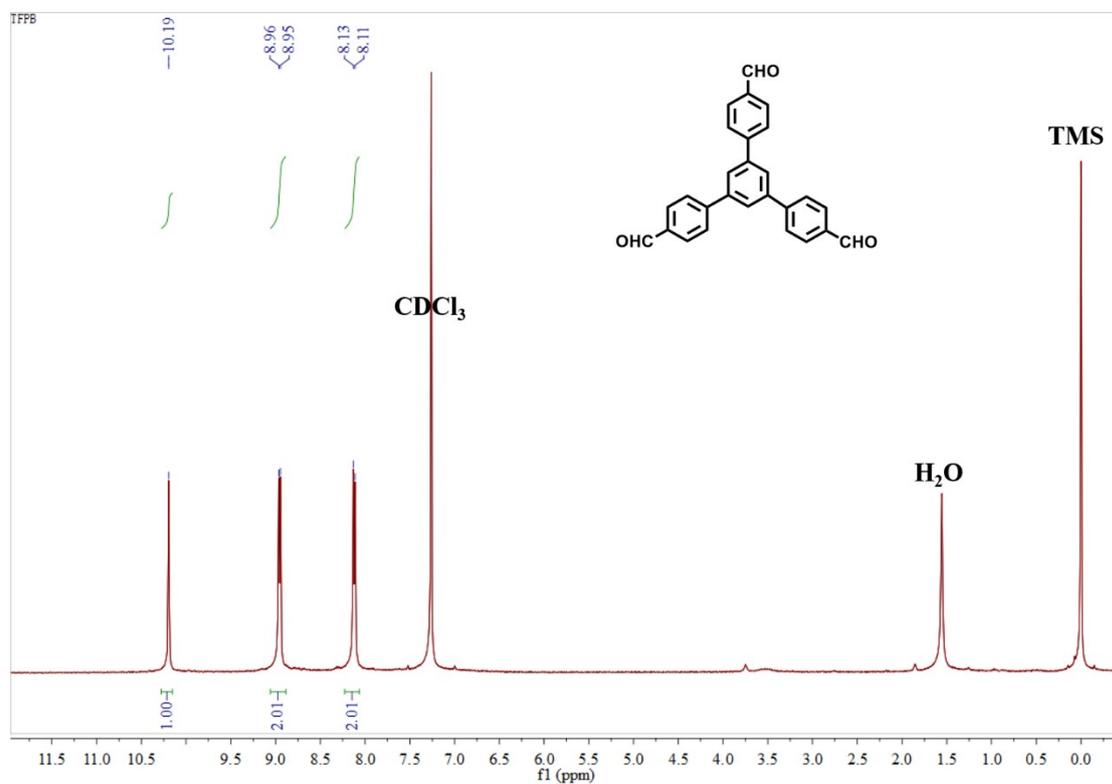
Fig. S2 ^{1}H NMR of 1,3,5-tris(4-formylphenyl)-benzene (TFPB) recorded in CDCl$_3$.
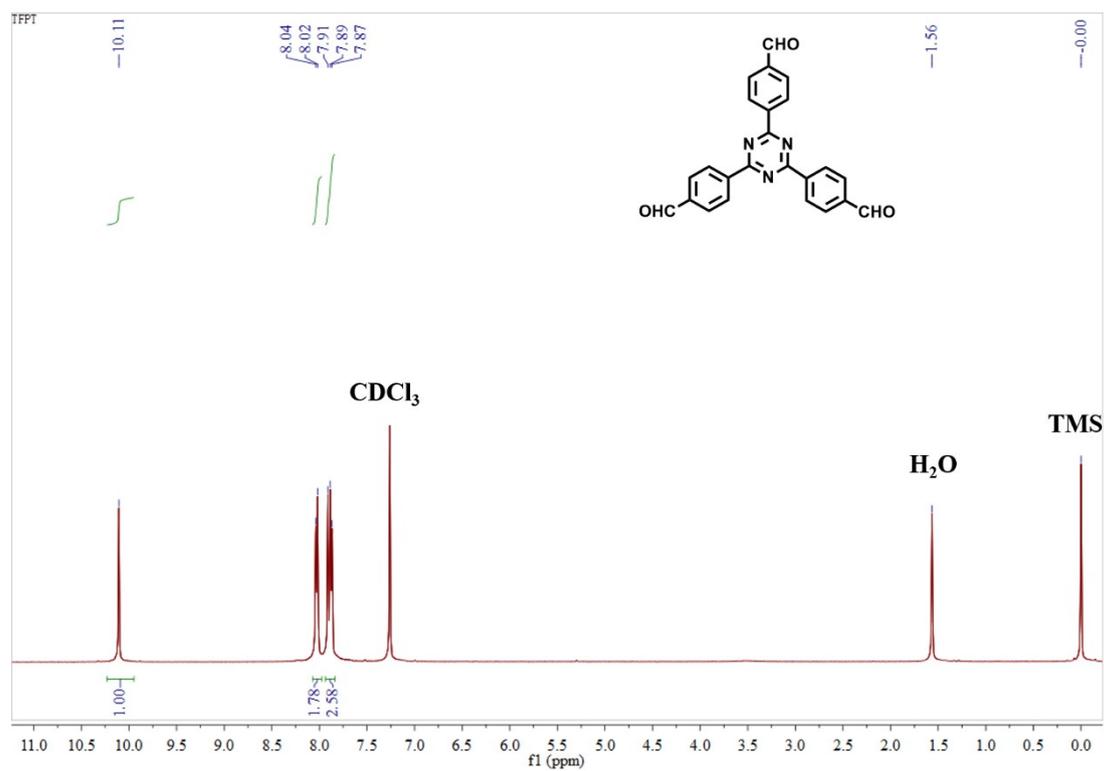
Fig. S3 ^{1}H NMR of 2,4,6-tris(4-formylphenyl)-1,3,5-triazine (TFPT) recorded in CDCl$_3$.
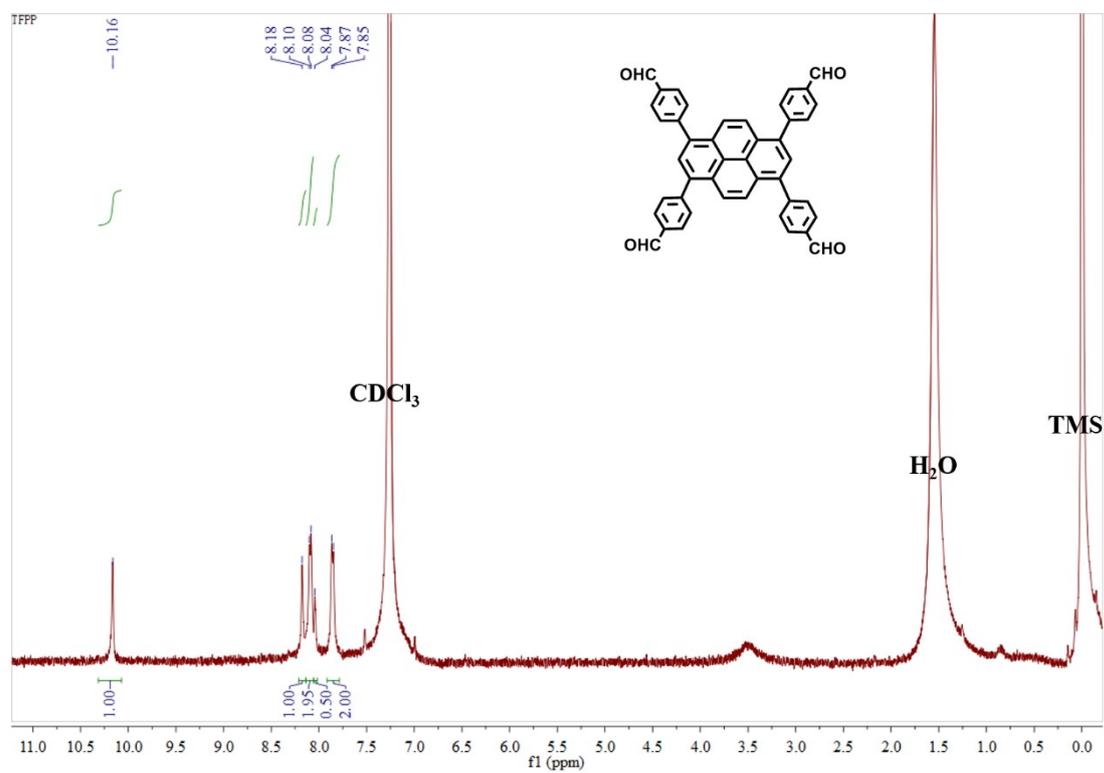
Fig. S4 ^{1}H NMR of 1,3,6,8-tetrakis(4-formylphenyl)-pyrene (TFPP) recorded in CDCl$_3$.
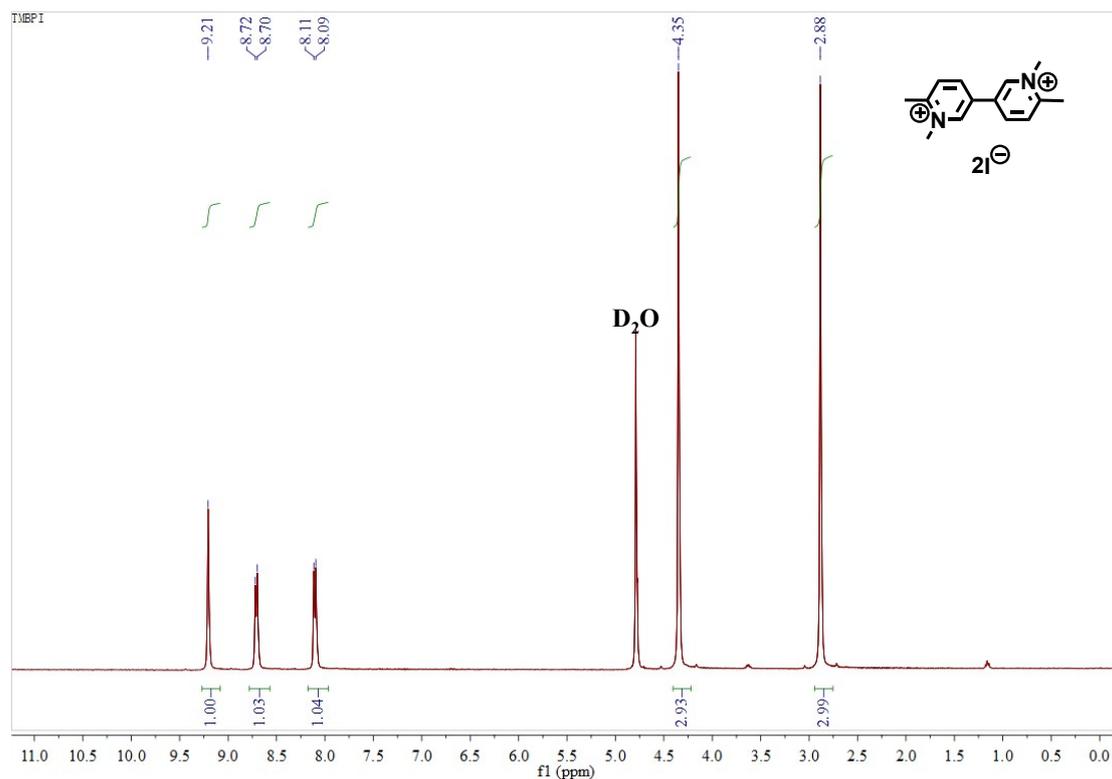
Fig. S5 ^{1}H NMR of 1,1',6,6'-tetramethyl-[3,3'-bipyridine]-1,1'-diium iodide (TMBPI) recorded in D$_2$O.
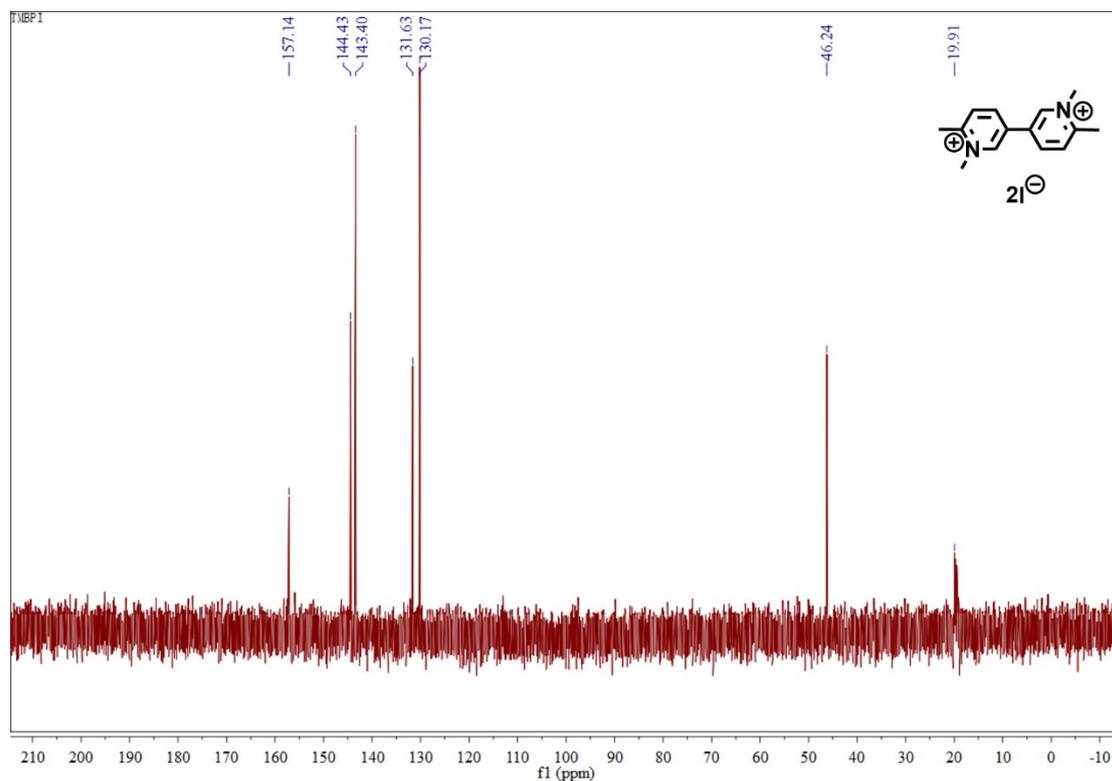
Fig. S6 ^{13}C NMR of 1,1',6,6'-tetramethyl-[3,3'-bipyridine]-1,1'-diium iodide (TMBPI) recorded in D$_2$O.

4. Other spectra and data
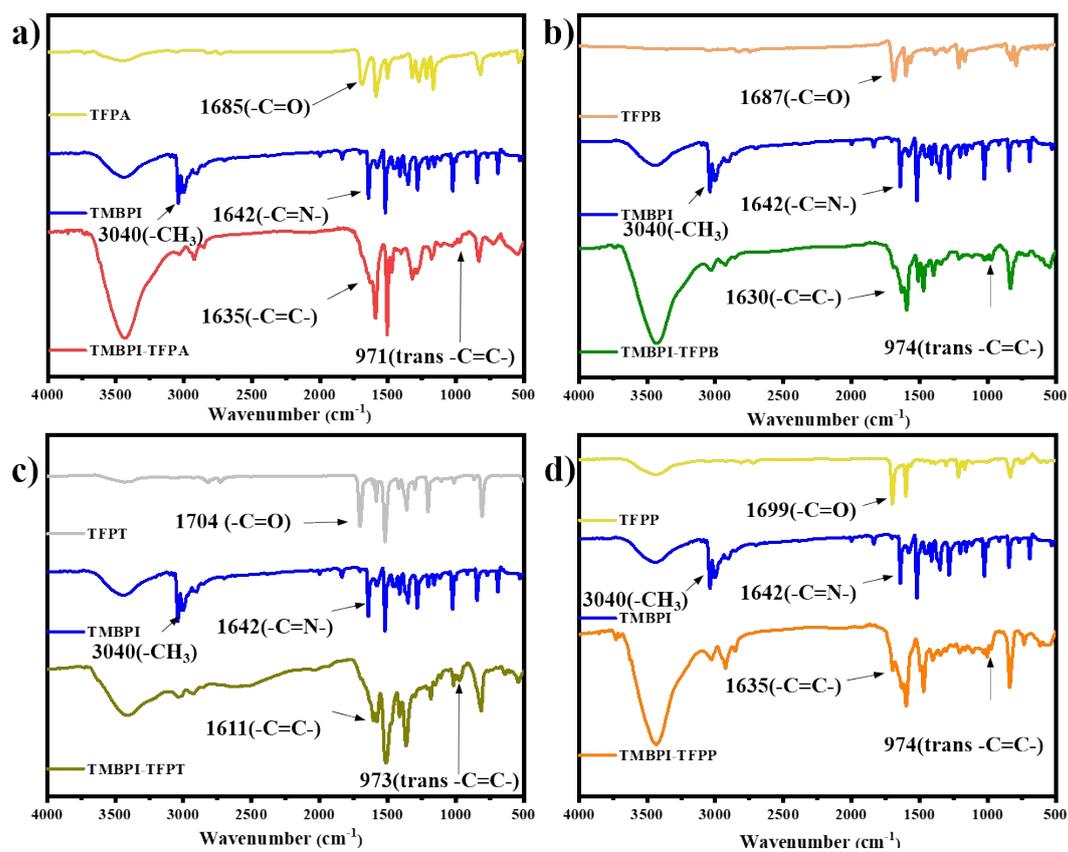
Fig. S7 FT-IR spectra of monomers and the porous polymers.
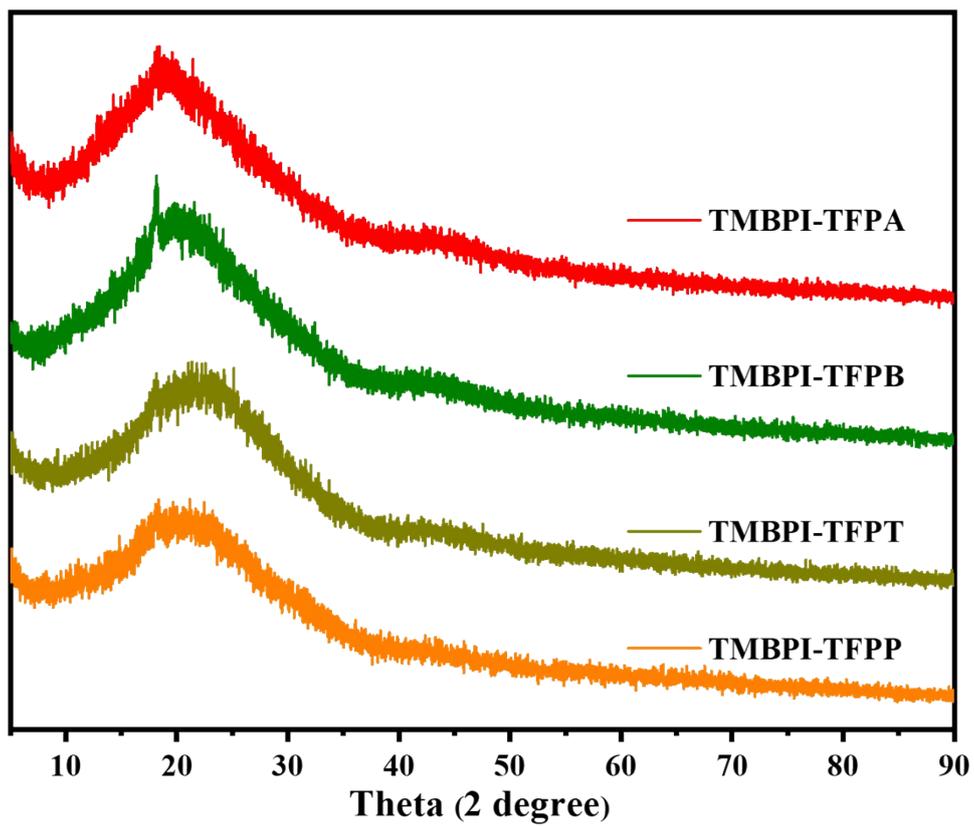
Fig. S8 PXRD patterns of the porous polymers.
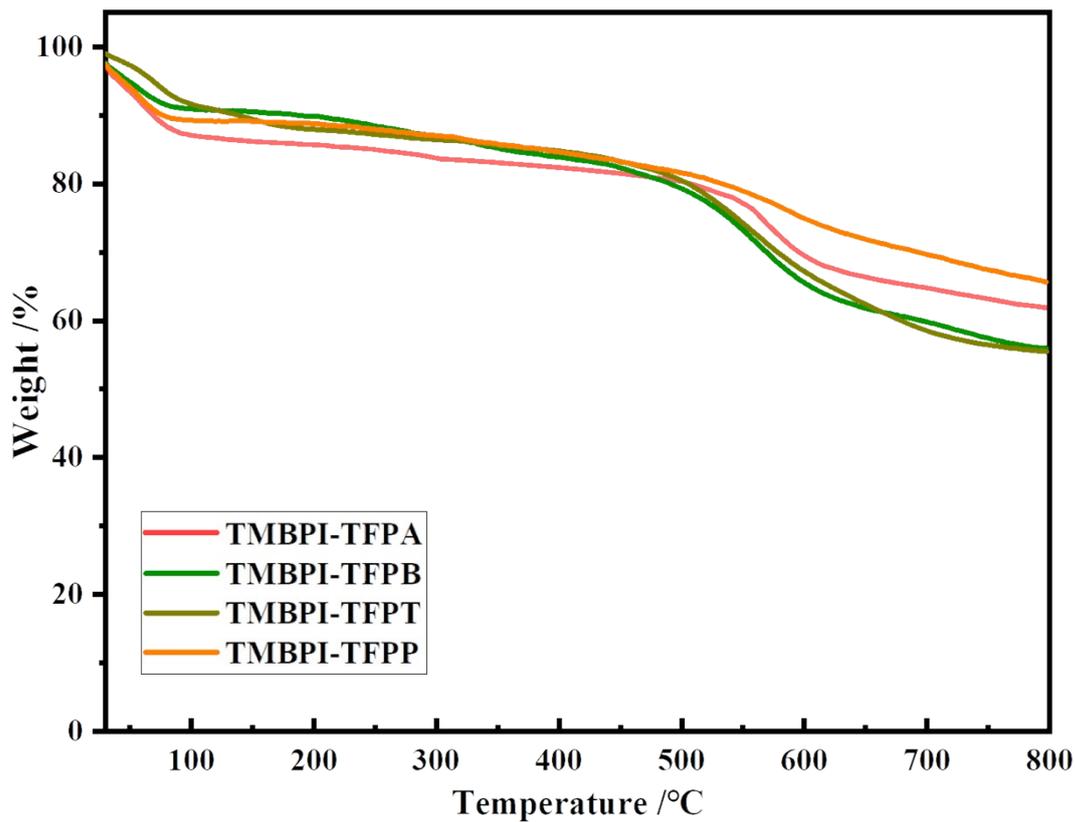
Fig. S9 Thermal gravimetric analysis (TGA) profiles of the porous polymers.
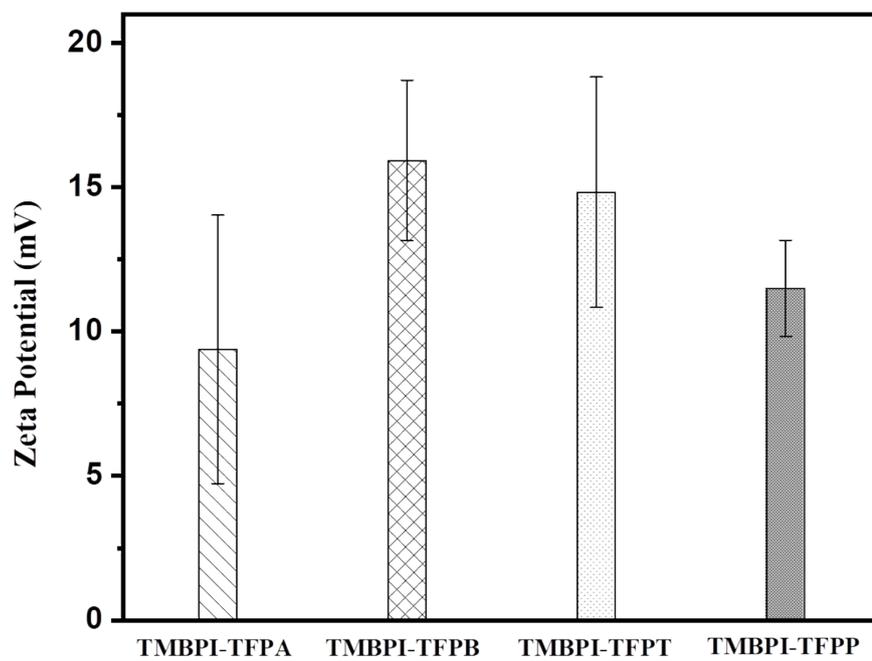
Fig. S10 The zeta potential of methanol dispersion of the porous polymers.
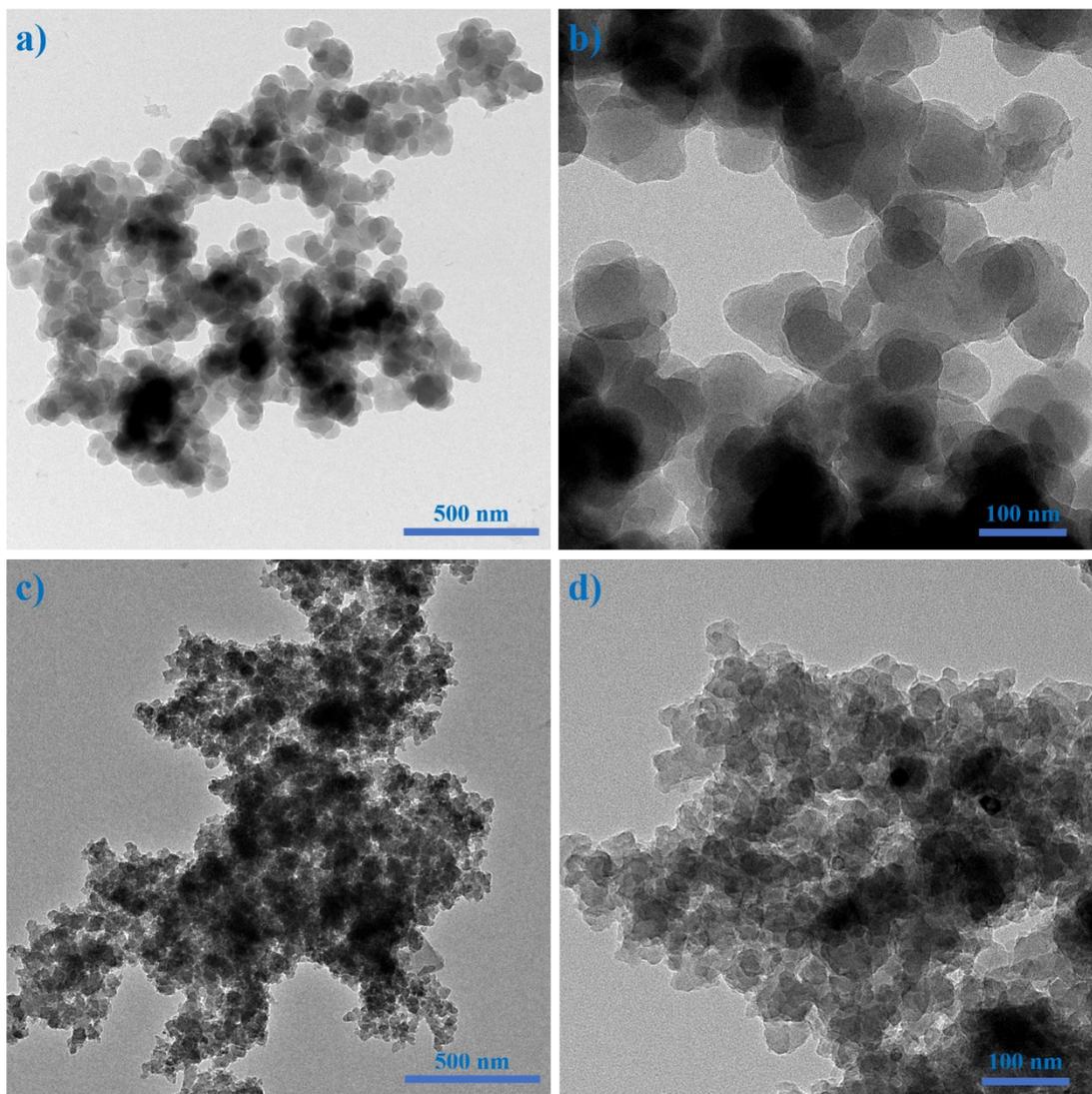
Fig. S11 TEM images of TMBPI-TFPA (a, b) and TMBPI-TFPB (c, d).
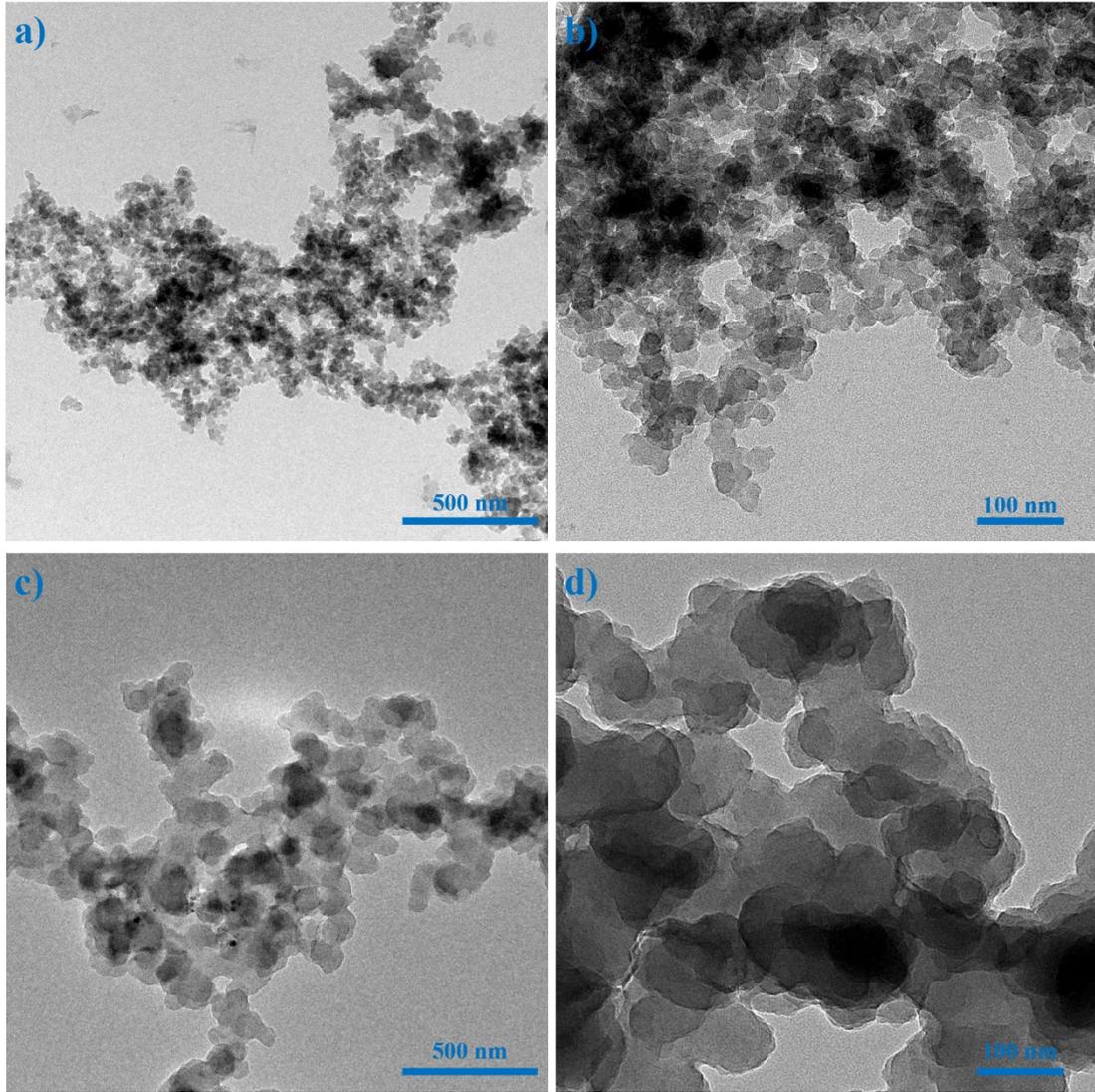
Fig. S12 TEM images of TMBPI-TFPT (a, b) and TMBPI-TFPP (c, d).
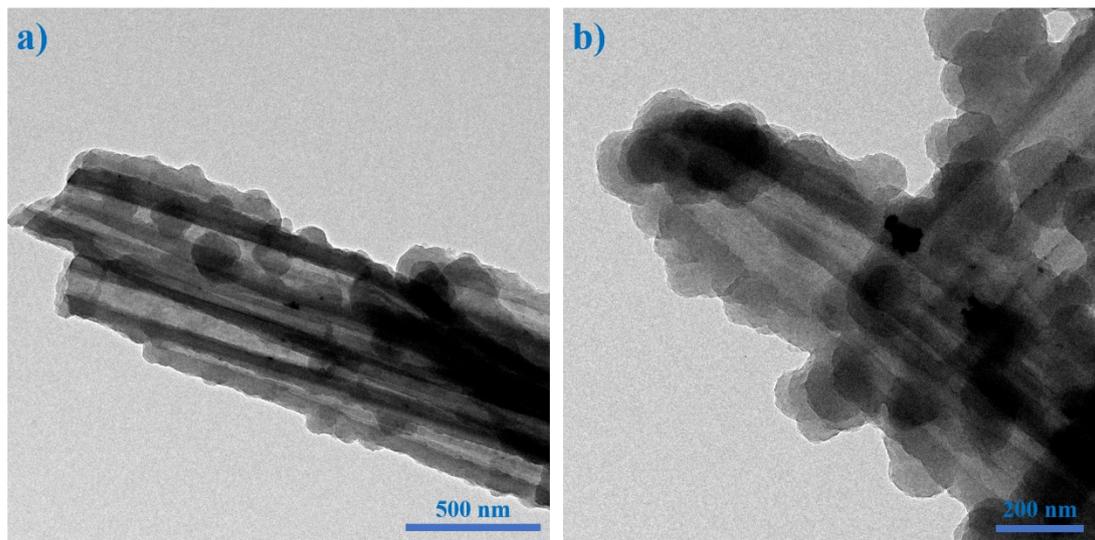
Fig. S13 TEM images of TMBPI-TFPP (a, b).

Table S1 Concrete data of antibacterial test of samples against E. *coli*

Sample \ Batch	1			2			3			4			5		
None	79	78	75	76	79	76	81	77	75	77	75	77	80	79	76
TMBPI-TFPA	34	30	30	31	34	29	30	32	34	32	32	31	35	30	34
TMBPI-TFPB	21	25	24	27	28	20	27	26	23	22	20	28	21	28	28
TMBPI-TFPT	29	24	25	27	26	28	27	26	24	22	24	28	29	26	24
TMBPI-TFPP	35	31	24	33	31	26	29	36	30	35	29	24	32	36	27

Table S2 Concrete data of antibacterial test of samples against S. *aureus*

Sample \ Batch	1			2			3			4			5		
None	71	74	73	73	75	70	73	71	72	72	72	75	70	75	70
TMBPI-TFPA	75	75	70	90	75	80	75	78	87	86	83	79	73	74	68
TMBPI-TFPB	103	101	101	113	107	110	110	111	109	105	105	120	100	110	105
TMBPI-TFPT	86	94	80	91	90	94	84	87	89	88	87	94	76	88	86
TMBPI-TFPP	108	118	114	104	123	127	119	113	111	117	113	129	126	119	115
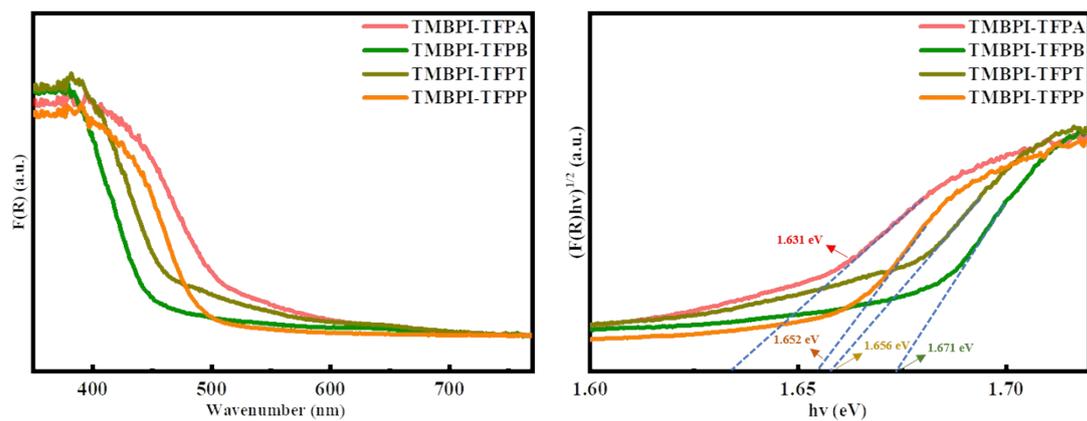
Fig. S14 (a) UV‑vis DRS of the porous polymers (b) Band gaps determined from the Kubelka‑Munk‑transformed reflectance spectra.
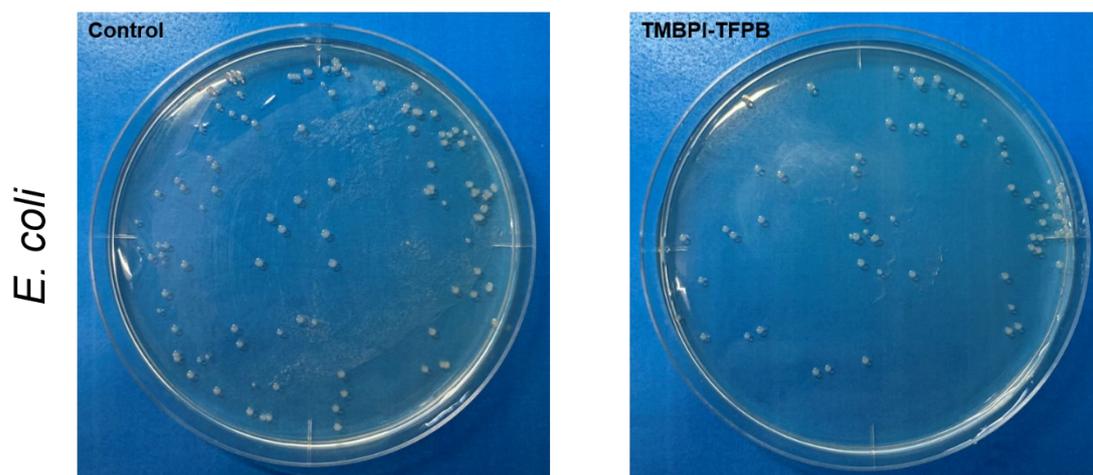
Fig. S15 Images of colony-forming cell assays against E. *coli*.
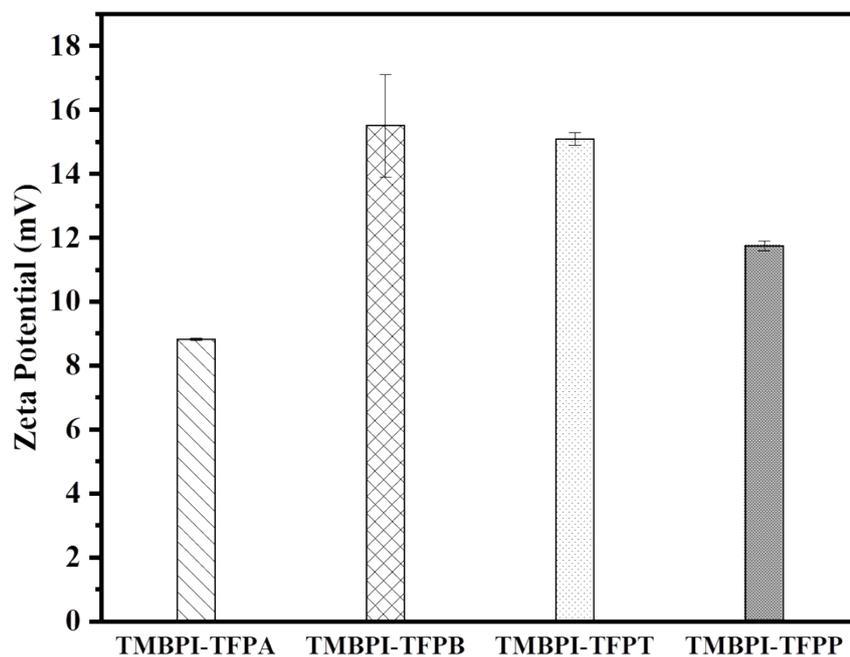
Fig. S16 The zeta potential of the porous polymers after the antibacterial tests.
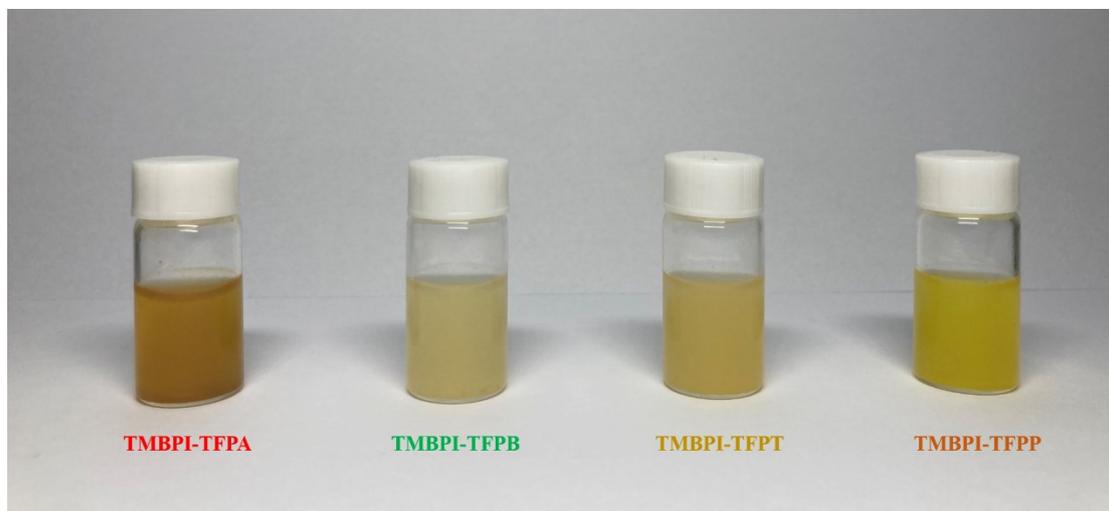
Fig. S17 Digital photograph of the water dispersion of the as-prepared polymers after keeping still for 12 hours (0.25 mg/mL).

5. Supplementary references

1. S. Bi, C. Yang, W. Zhang, J. Xu, L. Liu, D. Wu, X. Wang, Y. Han, Q. Liang and F. Zhang, *Nature Communications*, 2019, **10**, 2467.

2. S. Wei, F. Zhang, W. Zhang, P. Qiang, K. Yu, X. Fu, D. Wu, S. Bi and F. Zhang, *Journal of the American Chemical Society*, 2019, **141**, 14272-14279.

3. K. Yu, S. Bi, W. Ming, W. Wei, Y. Zhang, J. Xu, P. Qiang, F. Qiu, D. Wu and F. Zhang, *Polymer Chemistry*, 2019, **10**, 3758-3763.

4. F. Zhang, S. Wei, W. Wei, J. Zou, G. Gu, D. Wu, S. Bi and F. Zhang, *Science Bulletin*, 2020, **65**, 1659-1666.

5. M. G. Rabbani, A. K. Sekizkardes, O. M. El-Kadri, B. R. Kaafarani and H. M. El-Kaderi, *Journal of Materials Chemistry*, 2012, **22**, 25409-25417.

6. L. Ascherl, E. W. Evans, M. Hennemann, D. Di Nuzzo, A. G. Hufnagel, M. Beetz, R. H. Friend, T. Clark, T. Bein and F. Auras, *Nature Communications*, 2018, **9**, 3802.

7. T.-C. Lin, W.-L. Lin, C.-M. Wang and C.-W. Fu, 2011, **2011**, 912-921.

8. K. Wang, L.-M. Yang, X. Wang, L. Guo, G. Cheng, C. Zhang, S. Jin, B. Tan and A. Cooper, 2017, **56**, 14149-14153.

9. A.-J. Attias, C. Cavalli, B. Bloch, N. Guillou and C. Noël, *Chemistry of Materials*, 1999, **11**, 2057-2068.

10. S. Rizzo, S. Arnaboldi, V. Mihali, R. Cirilli, A. Forni, A. Gennaro, A. A. Isse, M. Pierini, P. R. Mussini and F. Sannicolò, 2017, **56**, 2079-2082.